STRUCTURE AND DYNAMICS OF ONE-DIMENSIONAL IONIC SOLUTIONS IN BIOLOGICAL TRANSMEMBRANE CHANNELS

ARNE SKERRA AND JÜRGEN BRICKMANN
Institut für Physikalische Chemie, Technische Hochschule Darmstadt, D-6100 Darmstadt, West Germany

ABSTRACT The structure and dynamics of solvated alkali metal cations in transmembrane channels are treated using the molecular dynamics simulation technique. The simulations are based on a modified Fischer-Brickmann model (Fischer, W., and J. Brickmann, 1983, *Biophys. Chem.*, 18:323–337) for gramicidin A–type channels. The trajectories of all particles in the channel as well as two-dimensional pair correlation functions are analyzed. It is found from the analysis of the stationary simulation state that one-dimensional solvation complexes are formed and that the number of water molecules in the channel varies for different alkali metal cations.

INTRODUCTION

There were several attempts in the last few years to explain the cation selectivity of gramicidin A–type transmembrane channels by microscopic models. Ion transport through the gramicidin A channel can be subdivided into three distinct processes: (*a*) diffusion of the ion from the bulk of the aqueous solution to the pore mouth (association step); (*b*) translocation of the ion through the channel; and (*c*) exit of the ion from the apposite channel mouth (dissociation step). Although some experimental investigations suggest that entry of the ion into the channel is the rate-determining step for transmembrane diffusion, it is not clear whether the intrachannel translocation process also contributes significantly. This latter process is an important example of a quasi one-dimensional diffusion process in nature and justifies a detailed study. It is particularly interesting to know whether the intrachannel diffusion shows selectivity for different alkali metal ions, which then may contribute to the selectivity of the entire transmembrane transport process.

It was already noted by Brickmann and Fischer (2) that the selectivity sequence for the intrachannel transport of alkali metal cations through gramicidin A–type model channels may be related to the effective mass of the transported particles, which is much higher than the mass of the isolated ion. This increase was related to the formation of hydration complexes. Experimental evidence for the presence of water inside the gramicidin A transmembrane channel were given by several authors (3–5).

The aim of this investigation is to study the solvation structure and its dynamical change in gramicidin A–type channels using the molecular dynamics technique. This method was used in several previous studies concerning the gramicidin A transmembrane channel (see reference 36 for an overview). In one of the first studies of this type, by Fischer et al. (1, 6), the presence of water molecules was completely neglected, and in one case the ion motion was restricted to the channel axis (6). Kappas et al. (7) considered the interactions between ion and water molecules inside the pore using an isotropic model of water, so the dipole properties of water could not be considered. Aityan and Chizmadgev (8) merely investigated the motion of water molecules inside the channel in the absence of an ion. The molecular dynamics studies of Mackay et al. (9) and Kim et al. (10) are of special interest because they explicitly included the complete atomic structure of gramicidin A in their computations. In both studies, however, the simulated time period of 5 and 0.5 ps, respectively, was too short for an observation of characteristic events like position changes of the ion and for the elucidation of the role of water molecules in the transport process.

Before investigating ion transport through gramicidin A–like transmembrane channels (see reference 9), it is necessary to study the structure and the dynamical behavior of the solvation complexes formed inside the ion channel. Particularly the number of water molecules occupying the pore must be known. As is shown in several experimental investigations, this number depends on the presence of an ion in the channel (11–13). Electrokinetic measurements reveal that in this case there are seven to nine water molecules inside the pore. Besides the varying statements concerning the number of water molecules, the

Dr. Skerra's present address is Zentrum für Gentechnologie, Am Klopferspitz, D-8033 Martinsried, FRG.

Correspondence should be addressed to Dr. Brickmann.

effective length of the ion channel for which these numbers are valid is not well defined. Therefore these experimental results are of limited scope for our calculations.

The number of water molecules occupying the pore must first be determined. To achieve this, the molecular dynamics simulation technique was applied, and reliable criteria for the elucidation of the number of water molecules were established.

An obvious criterion for the determination of the number of water molecules occupying the channel is the change of the physical pressure inside the pore when this number is varied. However, as was shown by Schäfer and Klemm (14), the calculation of physical pressure from molecular dynamics data does not give reliable values and was therefore not applied here.

Here we investigate the structure formed by water inside the channel in the presence of an ion and the dependence of this structure on the number of water molecules. These structural studies open alternative criteria for the determination of the number of water molecules in the channel interior. The probability density of the water molecules in the spatial environment of the ion is carefully analyzed. Moreover, the individual trajectories of the particles are studied.

METHODS

Model Approach

The molecular dynamics simulations are based on a model that consists of a set of particles representing the inner surface of the ion channel, an ionic particle, and a varying number of water molecules. An appropriate description of the transmembrane channel for molecular dynamics simulations is a central problem. If all atoms in the gramicidin A ion channel are considered in evaluating the interaction energies, the computer time is drastically increased, which results in a strong limitation of the simulated time period (9, 10). Instead, we chose the simplified model channel, developed by Fischer and Brickmann (6), which possesses the essential features of the interior of a gramicidin A–type ion channel.

For our present work we improved the model in important details. First, the model was completely reparameterized based on Urry's gramicidin A atomic coordinates (15). In addition to the previously single torsional vibration mode of the carbonyl groups, two more vibrational modes were introduced.

The protein channel is modeled by a hexagonal helical arrangement of dipoles (Fig. 1) that represent the carbonyl groups of the peptide bonds at the interior of the gramicidin A channel. The dipoles consist of two mass points each, one for the carbon and one for the oxygen atom. The carbon atoms are arranged on a rigid helix with five turns, six atoms per single turn. Such a rigid structure is justified by the experimental investigations of Wallace et al. (16, 17) and Naik and Krimm (18), who found that the conformational changes of gramicidin A when binding a cation are insignificant. Moreover, we did not explicitly consider the influence of possible conformational changes of the model channel interior.

The oxygen atoms are located in their equilibrium orientations (neglecting mutual interactions) in identical distances to the respective carbon atoms. The dipoles form an equilibrium angle with the channel axis, the value of which alternates between 17.5° and 162.5°.

The geometry of the model was obtained by least square fit methods from Urry's gramicidin A atomic coordinates (15).

The carbonyl groups of the model channel possess three vibrational modes representing the in-plane and out-of-plane torsional modes and the

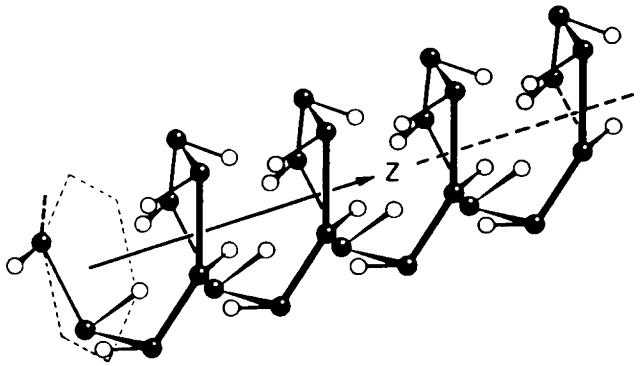

FIGURE 1 Helical arrangement of carbonyl groups in the channel model (schematically).

stretching mode of the C—O bond. The harmonic potentials of these modes are defined by placing the origin of a local polar coordinate system in each of the carbon atoms. The plane for $\vartheta = 90°$ corresponds to the plane through the respective carbon atom and the channel axis. The equilibrium position of the oxygen atom is characterized by $\Phi = 0°$, $\vartheta = 90°$, and $d = d_0$. The potential energy due to these three vibrational modes is defined as follows:

$$V = \frac{k_\Phi}{2}\Phi^2 + \frac{k_\vartheta}{2}(\vartheta - 90°)^2 + \frac{k_d}{2}(d - d_0)^2.$$

The torsional modes according to Φ and ϑ stand for the out-of-plane and the in-plane bending mode of the peptide carbonyl group. The stretching mode defined by d corresponds to the C—O valency mode.

The mutual interactions of the carbonyl groups as well as the interactions between the carbonyl groups and the particles inside the pore (ion and water molecules) are due to electrostatic and van-der-Waals forces. This leads to a strong anharmonic coupling of the dipole vibrational modes and therefore to a fast energy dissipation among the vibrational degrees of freedom.

The electrostatic interactions are described by a Coulomb potential with the carbon atoms bearing a charge of $+q$ and the oxygen atoms bearing a charge of $-q$.

The van-der-Waals interactions are represented by Lennard–Jones (6, 12) potential functions:

$$V(r) = 4\epsilon[(\sigma/r)^{12} - (\sigma/r)^6].$$

The Lennard–Jones parameters for interactions between atoms of different types are evaluated by applying the Lorentz–Berthelot combination rule (19). All parameters are given in Table I.

The van-der-Waals repulsion between the carbonyl groups and the particles inside the pore are sufficient to constrain these particles to the channel interior. Thus it is not necessary to impose an artificial repulsive potential around the channel as in the previous model (1). Because of this fact we believe that the influences of the amide groups and of the amino acid alpha carbon atoms are of minor influence on the behavior of the channel interior. The additional omission of the amino acid side chains in our model only has the effect that we cannot consider possible polarizability influences of these groups.

To describe the water–water interactions, the TIP4P model introduced by Jorgensen et al. (20) was chosen. It consists of four force centers that are arranged in a rigid structure as shown in Fig. 2. Three of them are located at the positions of the two hydrogen atoms and the position of the oxygen atom, respectively. The fourth center, M, with zero mass is located on the bisector between the two O—H bonds.

At the positions of the hydrogen atoms and point M, there are electrical charges resulting in Coulomb interactions between the water molecules themselves and interactions between the water molecules and the ion or the carbonyl groups.

TABLE I
PARAMETERS OF THE MODEL CHANNEL

Radius of the helix	$.337 \cdot 10^{-10}$ m
Pitch of the helix h	$4.58 \cdot 10^{-10}$ m
Periodicity length	$22.9 \cdot 10^{-10}$ m
Equilibrium distance carbon–oxygen d_0	$1.24 \cdot 10^{-10}$ m
Equilibrium angles of the carbonyl groups with respect to the channel axis	17.5° or 162.5°
Mass of the oxygen atom m_O	$2.656 \cdot 10^{-26}$ kg
Partial charge of the carbon atom q_C*	$0.609 \cdot 10^{-19}$ C
Partial charge of the oxygen q_O*	$-0.609 \cdot 10^{-19}$ C
Lennard–Jones parameters for carbon*	
CC	$3.617 \cdot 10^{-10}$ m
CC	$1.028 \cdot 10^{-21}$ J
Lennard–Jones parameters for oxygen	
OO	$2.86 \cdot 10^{-10}$ m
OO	$1.584 \cdot 10^{-21}$ J
C—O stretching mode‡	
Force constant k_d	$1.003 \cdot 10^3$ J/m^2
Wave number	1,032 cm^{-1}
In-plane binding mode of the C—O group‡	
Force constant k	$1.25 \cdot 10^{-18}$ J
Wave number	293 cm^{-1}
Out-of-plane binding mode of the C—O group‡	
Force constant k	$0.657 \cdot 10^{-18}$ J
Wave number	213 cm^{-1}

*From Mackay et al. (9).
‡From reference 37.

The oxygen position is a center of force for van-der-Waals interactions, which are evaluated by a Lennard–Jones potential function (20). Applying the Lorentz–Berthelot combination rule, the nonionic interactions between the carbonyl groups and the water molecules are depicted in the form of Lennard–Jones potentials as well. The parameters of the TIP4P model are listed in Table II.

The ion is subject to electrostatic and van-der-Waals interactions as are the other particles of the model. The electrostatic forces are represented by Coulomb potentials that act between the ion's center of mass and the centers of force of the carbonyl groups as well as those of the water molecules.

Concerning the nonionic interactions, we distinguish between the interactions of the ion with the carbonyl groups on one hand and those with the water molecules on the other hand.

The van-der-Waals interactions between the ion and the atoms of the carbonyl groups are described again by Lennard–Jones potentials. The Lennard–Jones parameters are obtained from the individual parameters by applying the Lorentz-Berthelot combination rule.

To evaluate the van-der-Waals interactions between the ion and the water molecules, we chose potential functions that were deduced by Bounds et al. (21, 22) from the self consistent field (SCF) calculations by Kistenmacher et al. (23, 24) and Dacre (25, 26). Following Bounds et al., the entire nonionic interaction energy between the cation and a water molecule consists of one contribution that depends on the ion–oxygen

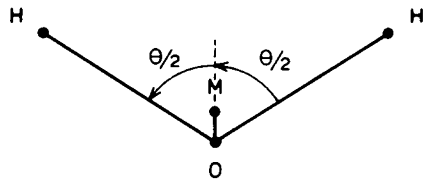

FIGURE 2 Force centers for the TIP4P-water model (21).

TABLE II
PARAMETERS OF THE TIP4P MODEL*

Oxygen–Hydrogen distance r_{OH}	$0.9572 \cdot 10^{-10}$ m
H—O—H angle θ	104.52°
M—O distance r_{OM}	$0.15 \cdot 10^{-10}$ m
Oxygen mass m_O	$2.656 \cdot 10^{-26}$ kg
Hydrogen mass m_H	$1.674 \cdot 10^{-27}$ kg
Partial charge of H atom q_H	$0.833 \cdot 10^{-19}$ C
Partial charge at point M q_M	$-1.666 \cdot 10^{-19}$ C
Lennard–Jones parameters	
σ_{WW}	$3.15 \cdot 10^{-10}$ m
ϵ_{WW}	$1.08 \cdot 10^{-21}$ J

*From Jorgensen et al. (20).

distance r_{IO}

$$V(r_{IO}) = A_{IO} \exp(-b_{IO} r_{IO}) - C_{IO}/r_{IO}^4 - D_{IO}/r_{IO}^6,$$

and two contributions that depend on the ion–hydrogen distance r_{IH}

$$V(r_{IH}) = A_{IH} \exp(-b_{IH} r_{IH}).$$

The atomic coordinates used in this description are identical with the respective positions in the TIP4P model. The ion-specific parameters A_{IO}, b_{IO}, C_{IO}, D_{IO}, A_{IH}, and b_{IH} are given in Table III. This representation of the nonionic interactions between cation and water molecules is consistent with the Coulomb interaction between the ion and the charge distribution in the TIP4P model, as described above. Compared with the Lennard–Jones potential functions, this representation is advantageous because the numerical error made by applying combination rules is avoided. The potentials have been tested in molecular dynamics simulations (22), which gave reasonable results for the solvation of the alkali metal ions in aqueous solution.

Molecular Dynamics Simulation Technique

This work is focused on the particle diffusion processes inside the pore. To avoid boundary effects, periodic boundary conditions were introduced in the direction of the channel axis (27, 28). Due to the periodic boundary

TABLE III
PARAMETERS FOR THE INTERACTION BETWEEN THE IONS AND WATER MOLECULES AND THE ION CHANNEL

	Li^+	Na^+	K^+
Mass of the ion m_I (10^{-26} kg)	1.165	3.818	6.470
Charge of the ion q_I (10^{-19} C)	1.602	1.602	1.602
Lennard–Jones parameters*			
II (10^{-10} m)	2.75	2.94	3.46
II (10^{-23} J)	0.58	8.10	41.70
Parameters for the interaction of the ions with water molecules‡			
A_{IO} (10^{-16} J)	0.8704	1.900	3.744
b_{IO} (10^{10} m^{-1})	3.394	3.546	3.339
C_{IO} (10^{-58} J m^4)	2.855	3.022	3.043
D_{IO} (10^{-78} J m^6)	−2.654	−5.836	−4.433
A_{IH} (10^{-17} J)	1.262	1.434	3.993
b_{IH} (10^{10} m^{-1})	3.980	3.394	3.413

*From reference 38.
‡From references 21 and 22.

conditions, a cut-off radius of 1.1 nm was used for all nonbonding interactions. To maintain poor conservation of the total energy, the method of shifted force potentials developed by Streett et al. (29, 30) was applied.

The interactions described above lead to a system of coupled translational and rotational equations of motion. These equations were solved using the predictor corrector scheme developed by Gear (31). The forces due to the oscillations of the carbonyl groups were transformed into cartesian coordinates to reduce the numerical effort. The rotations of the rigid water molecules were described using the quaternion parameters introduced by Evans (32, 33). The rotational equations of motion were solved applying a formalism developed by Sonnenschein (34).

The simulations were carried out with a time step length of $1.0 \cdot 10^{-15}$s. All simulations were performed at a temperature of 298 ± 10 K. The period of simulation was in each case 100 ps, corresponding to 100,000 time steps.

Pair Correlation Functions

Our aim is to study the structure formed by the water molecules inside the pore. An appropriate method is the evaluation of the pair correlation functions between the ion and the water molecules. When defining the relative spatial coordinates between the ion and the water molecules for this function, it is helpful to consider the special symmetry properties of the ion channel. For this purpose we define a cylinder coordinate system with its origin at the actual position of the ion, the z-axis of which is always parallel to the channel axis.

The z value is therefore given as the projection of the distance between the ion and the oxygen of a water molecule on the channel axis. ρ is the distance of this oxygen to the z axis of the cylinder coordinate system (Fig. 3). The spatial orientations of the water molecules are neglected. The probability density is evaluated by adding the z- and ρ-values every fifth time step, resulting in the function $\tilde{g}(z, \rho)$. The pair correlation function is obtained by scaling as follows:

$$g(z, \rho) = \tilde{g}(z, \rho) \Big/ \left(2\pi\Delta z \cdot \Delta\rho \cdot N_I \cdot \frac{N_w}{V} \cdot n\right).$$

The value of both Δz and $\Delta\rho$ is $0.2 \cdot 10^{-10}$ m, N_I equals 1, and n is the number of summations. N_w/V is determined according to a water density of 1 g/cm^3.

RESULTS AND DISCUSSION

To determine the number of water molecules inside a gramicidin A–type channel in the presence of Li^+, Na^+, or K^+, we first performed molecular dynamics simulations with Na^+ and six to nine water molecules. The pair correlation functions that we obtained are displayed in Figs. 4–7 in a three-dimensional representation.

A striking feature of these diagrams is the well defined

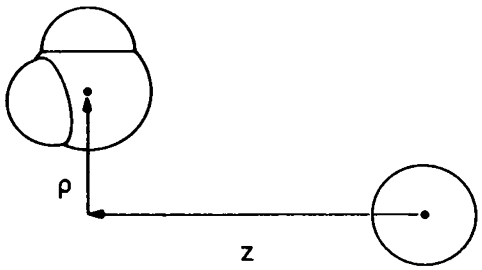

FIGURE 3 Cylinder coordinate system for the ion–water correlation function $g(z, \rho)$.

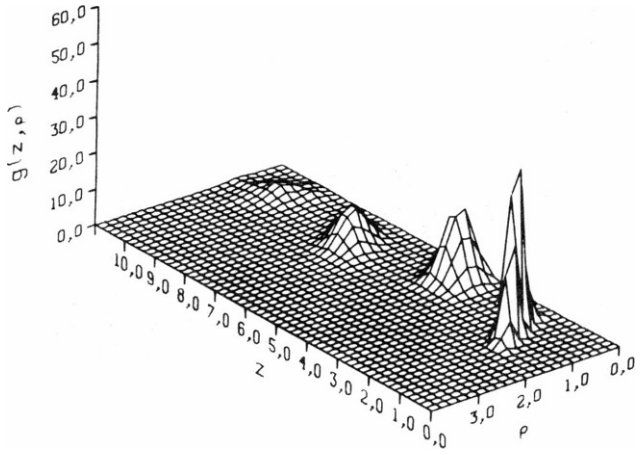

FIGURE 4 Pair correlation function for six water molecules in the channel in the presence of a sodium ion.

appearance of the probability density maxima. This leads to the conclusion that the water molecules form a highly ordered structure relative to Na^+. The water molecules are obviously arranged in an angled chain in the direction of the channel axis, one site being occupied by the ion instead of a water molecule. Na^+ is directly coordinated by two water molecules. These coordinating water molecules account for the highest peak in the diagrams, which is closest to the origin of the coordinate system. The remaining coordination sites of the ion are partially occupied by the oxygen atoms of the channel carbonyl groups. The second water maximum is of comparable amplitude to the first one, independent of the number of water molecules in the pore. This shows that the ion is coupled to at least four water molecules (two on each side of the ion) during the whole simulation period.

To optimize the solvation shell the qualitative behavior of the third and fourth maximum was studied in raising the number of water molecules from six to eight. The positions of these peaks remain unchanged; only their amplitude grows. This indicates that there are eight binding positions

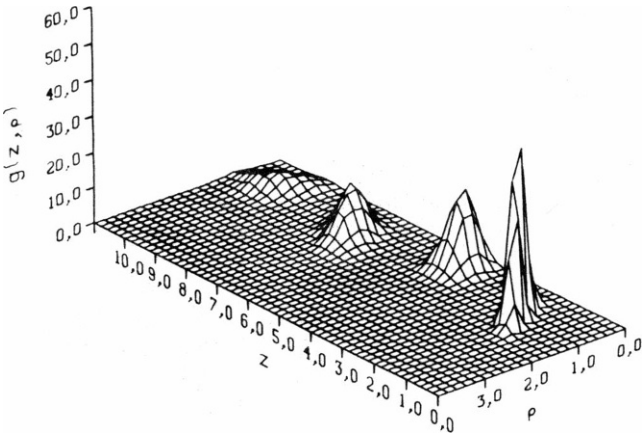

FIGURE 5 Pair correlation function for seven water molecules in the channel in the presence of a sodium ion.

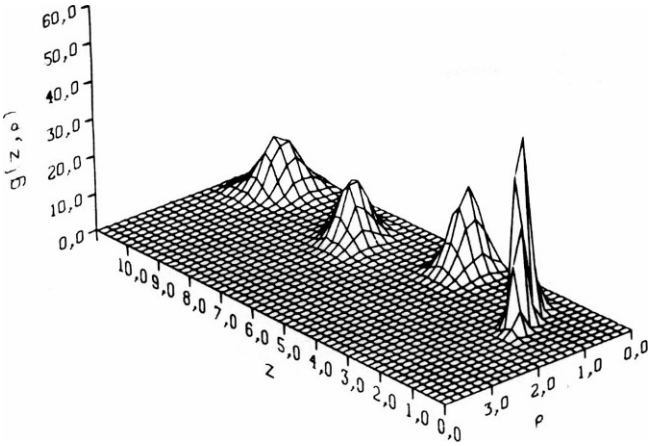

FIGURE 6 Pair correlation function for eight water molecules in the channel in the presence of a sodium ion.

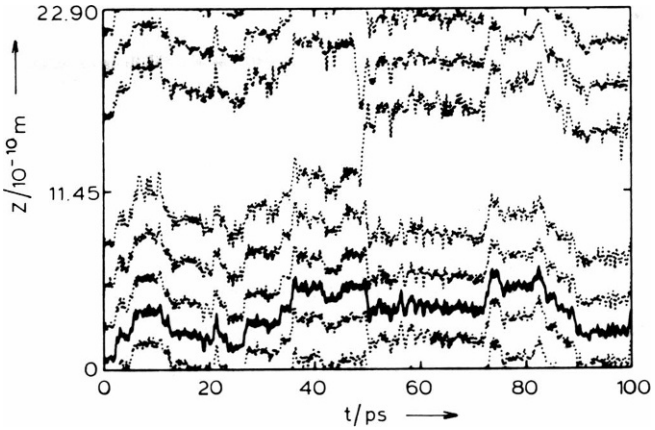

FIGURE 8 Projection of the trajectories of a sodium ion and six water molecules on the channel axis Z as resulting from the molecular dynamics simulation. *Solid line*, ion; *dotted line*, water molecules.

relative to the ion even if the number of water molecules is smaller than eight. These binding positions are successively occupied when the number of water molecules is increased from six to eight, but they are not shifted.

A completely different behavior is observed when there are nine water molecules placed inside the channel. The water chain becomes more angled. A fifth peak arises.

We conclude from this observation that up to eight water molecules occupy sites that have a well defined geometric arrangement with respect to the ion. With eight molecules in the pore all sites are filled, i.e., the solvation shell is completed. If an additional water molecule is placed into the channel, the previous structure is strongly disturbed. Such an arrangement can only be realized by an enormous increase of the pressure acting on the molecules in the channel. Under physiological conditions, there is no obvious reason for the existence of such a pressure-induced structure.

In contrast, it is improbable that the pore is occupied by less than eight water molecules, resulting in vacant binding sites. This assumption is supported by the experimentally observed high proton permeability of the gramicidin A channel (5). This phenomenon is explained by a Grotthus-like mechanism, which is possible only if the water molecules form a continuous phase inside the channel (3).

These conclusions are supported by the records of the trajectories of the particles. The trajectories are given for six to nine water molecules in Figs. 8–11. The diagrams are obtained by drawing the z coordinates (with the z axis being identical with the channel axis) of the particles against time.

In the case of six as well as seven water molecules, a large gap between the otherwise equally spaced water trajectories becomes obvious. There are even spatial rearrangements to be observed around the gap. With eight water molecules inside the channel, the previously described gap vanishes completely. In contrast, with nine water molecules the mobility of the particles is significantly decreased. The water structure becomes artificially frozen.

Our observations give evidence that the channel is

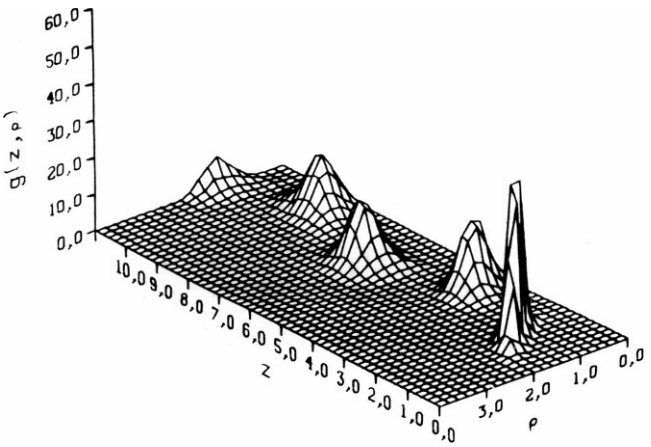

FIGURE 7 Pair correlation function for nine water molecules in the channel in the presence of a sodium ion.

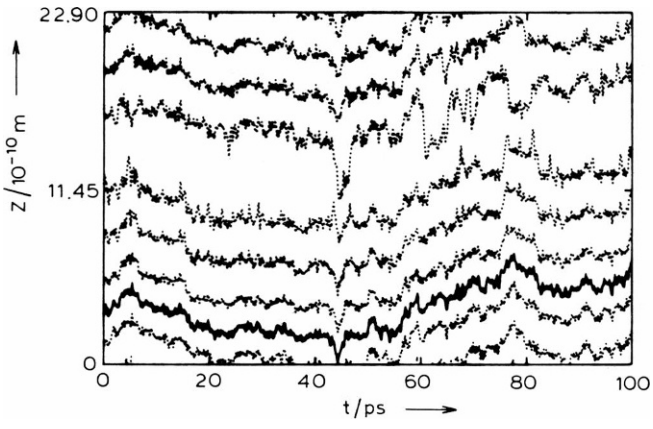

FIGURE 9 Projection of the trajectories of a sodium ion and seven water molecules on the channel axis Z as resulting from the molecular dynamics simulation. *Solid line*, ion; *dotted line*, water molecules.

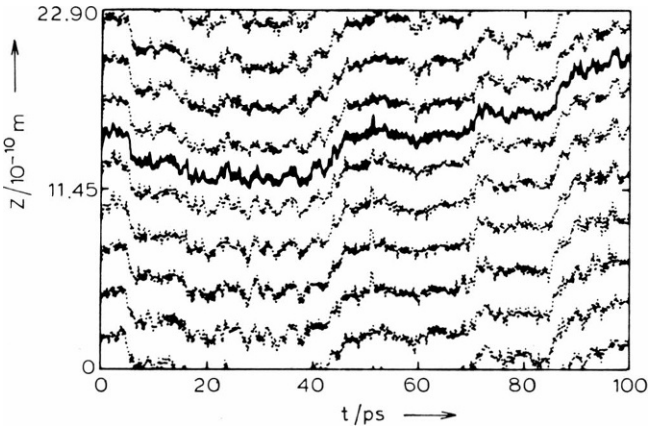

FIGURE 10 Projection of the trajectories of a sodium ion and eight water molecules on the channel axis Z as resulting from the molecular dynamics simulation. *Solid line*, ion; *dotted line*, water molecules.

occupied by eight water molecules in the presence of a sodium ion. The angled chain structure of the water molecules inside the pore can be explained by the fact that each water molecule forms a hydrogen bond towards the oxygen of a neighboring water molecule, whereas its second hydrogen atom interacts with a carbonyl oxygen. The structure formed in this way can be described as a one-dimensional aqueous solution.

This structure is highly consistent with the so-called single-file structure for the ion–water movement within the channel postulated by Finkelstein and Andersen (3) in their experimental results (3). The single-file model describes an almost linear arrangement of the particles inside the channel, so that the particles cannot pass each other.

Our results are in remarkable agreement with the findings of Mackay et al. (9) and Kim et al. (10). Both groups performed molecular dynamics simulations, including the complete atomic structure of gramicidin A in their computations. This reveals that our simplifications are fully justified for the structure and the dynamical behavior of the particles inside the channel.

The frozen structure, which we observe with nine water molecules inside the channel, can be explained by the increased pressure within the pore, leading to stronger interactions between the channel interior and the carbonyl groups. In this case 10 particles (nine water molecules and one ion) occupy the channel. This results in a highly ordered periodic arrangement within the five single turns of the channel helix.

Our argumentation concerning the number of water molecules in the presence of Na^+ can also be applied in the cases of Li^+ and K^+.

According to the results obtained for Na^+, we performed a simulation study for Li^+, with eight water molecules inside the channel. We presumed that in the case of the smaller lithium ion, the number of water molecules can only be larger than eight. Obviously even with eight water molecules there are no gaps between the trajectories (Fig. 12). One can conclude from these findings that also in the presence of Li^+ only eight water molecules occupy the channel.

The pair correlation diagram for Li^+ with eight water molecules is given in Fig. 13. The first peak is higher and closer to the position of the ion than in the case of Na^+. This can be obviously explained by the smaller ionic radius of Li^+ relative to Na^+, which leads to a stronger hydration of Li^+.

Since the ionic radius of K^+ is larger than that of Na^+, we may assume that for K^+ the channel is occupied by less than eight water molecules. Indeed this can be shown by comparing the pair correlation diagrams obtained for seven and eight water molecules. Going from seven to eight water molecules the pair correlation functions change in a similar way as in the case of Na^+, when increasing the number of water molecules from eight to nine. Moreover, with seven water molecules in the presence of K^+, there are no gaps between the trajectories observed (Fig. 14). Thus

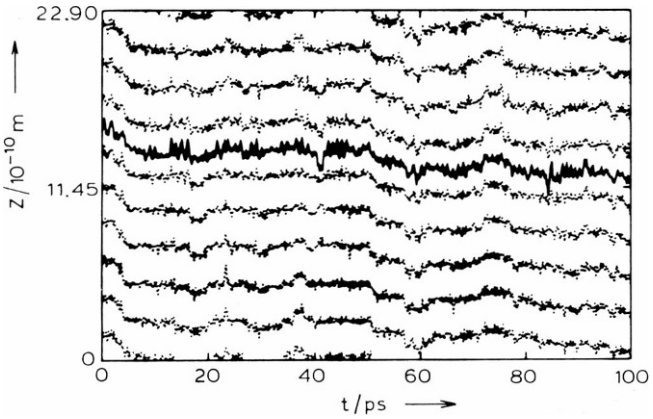

FIGURE 11 Projection of the trajectories of a sodium ion and nine water molecules on the channel axis Z as resulting from the molecular dynamics simulation. *Solid line*, ion; *dotted line*, water molecules.

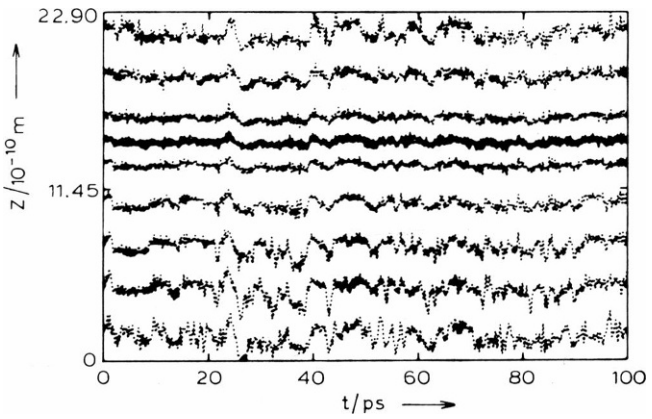

FIGURE 12 Projection of the trajectories of a lithium ion and eight water molecules on the channel axis Z as resulting from the molecular dynamics simulation. *Solid line*, ion; *dotted line*, water molecules.

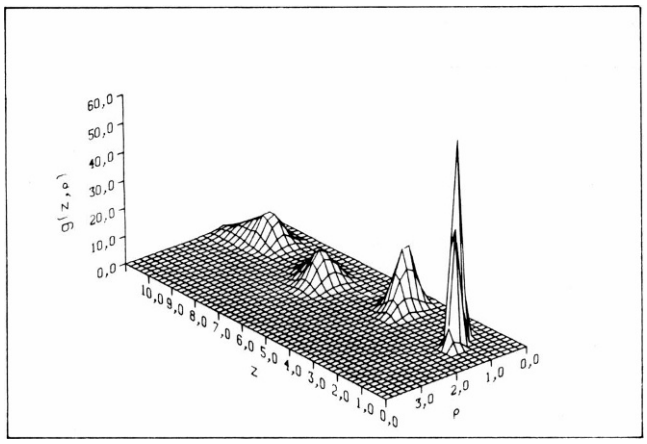

FIGURE 13 Pair correlation function for eight water molecules in the channel in the presence of a lithium ion.

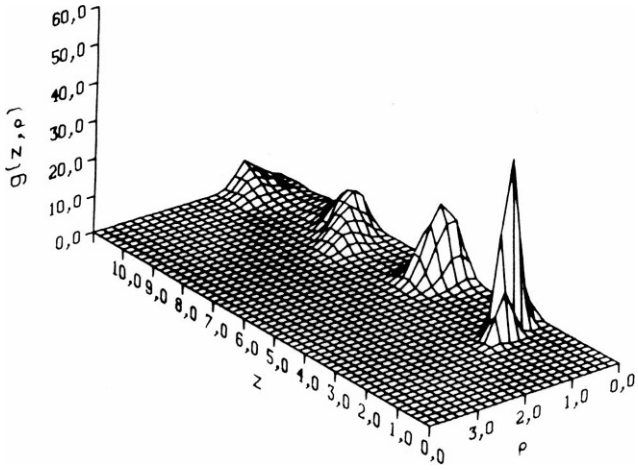

FIGURE 15 Pair correlation function for seven water molecules in the channel in the presence of a potassium ion.

K^+ is accompanied by seven water molecules inside the channel. The corresponding pair correlation function is given in Fig. 15. The first peak is lower and more distant from the origin as can be expected from the larger ionic radius of K^+ compared with Na^+.

There are two possible caveats concerning the above considerations. Both of them come from the application of periodic boundary conditions in the molecular dynamics simulations.

One restriction is that we can only place an integral number of water molecules inside the channel. Fractional numbers can only be introduced by increasing the periodicity length, leading to a drastic increase in the computational effort. However, the observation that for Li^+ and K^+ the water molecules with the largest distance from the ion have increased mobility indicates that fractional numbers of water molecules have only a weak influence on the dynamical properties of the ionic migration in the channel.

The second effect of the periodic boundary conditions follows from the opposite orientation of the water molecules at both sides of the ion. The consequence of this is that one water molecule must intereact with both ends of the so-formed water chains. We do not believe, however, that this effect significantly influences the results because the sum of interactions between the water molecules and polar channel groups dominates drastically the energetic effects of one "wrongly oriented" water molecule in the fourth "solvation shell" of the ion.

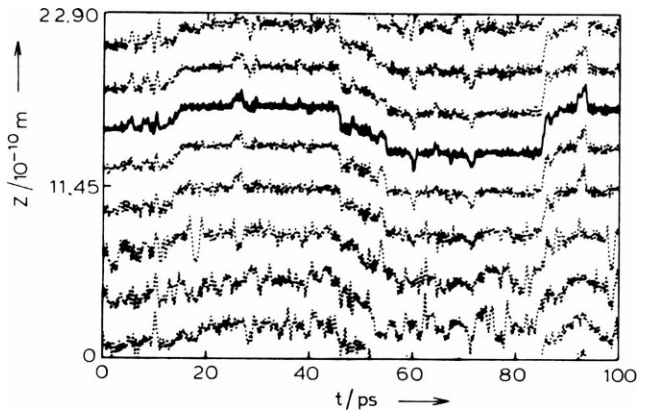

FIGURE 14 Projection of the trajectories of a potassium ion and seven water molecules on the channel axis Z as resulting from the molecular dynamics simulation. *Solid line*, ion; *dotted line*, water molecules.

CONCLUSION

The structure formed by the particles inside a gramicidin A–type model channel provided a plausible criterion for the determination of the number of water molecules within such a model pore. We could show that in the presence of Li^+ or Na^+, the channel is occupied by eight water molecules, whereas in the presence of K^+ there are seven water molecules in the pore. The most striking feature is the single-file structure formed by the ion and water molecules.

Due to the simulation period, which we were able to extend up to 100 ps, the entire equilibration of the system is guaranteed, whereas this is not certain for the works of other authors (9, 10). As was demonstrated by Brickmann and Fischer (2), the effective mass of an ion in the channel influences the selectivity sequence for the intrachannel diffusion. Consequently the determination of the solvation shell of the ion is a prerequisite for an adequate treatment of the ion migration on a microscopic basis. The single-file model, evaluated in this paper, will be used in a subsequent contribution to study the ionic flux in narrow channels in the presence of an external electric field (35).

We thank Dr. Wolfgang Stephan for helpful comments and carefully reading the manuscript.

A. Skerra thanks the Studienstiftung des Deutschen Volkes for financial support. This work was also supported by the Bundesminister für Forschung und Technologie, Bonn, and the Fonds der Chemischen Industrie, Frankfurt.

Received for publication 3 July 1986 and in final form 29 December 1986.

REFERENCES

1. Fischer, W., and J. Brickmann. 1983. Ion-specific diffusion rates through transmembrane protein channels. A molecular dynamics study. *Biophys. Chem.* 18:323–337.
2. Brickmann, J., and W. Fischer. 1983. Entropy effects on the ion-diffusion rate in transmembrane protein channels. *Biophys. Chem.* 17:245–258.
3. Finkelstein, A., and O. S. Andersen. 1981. The gramicidin A channel. A review of its permeability characteristics with special reference to the single-file aspect of transport. *J. Membr. Biol.* 59:155–171.
4. Hladky, S. B., and D. A. Haydon. 1984. Ion movements in gramicidin channels. Ion channels: molecular and physiological aspects. *Curr. Top. Membr. Transp.* 21:327–363.
5. Myers, V. B., and D. A. Haydon. 1972. Ion transfer across lipid membranes in the presence of gramicidin A. I. The ion selectivity. *Biochim. Biophys. Acta.* 274:313–322.
6. Fischer, W., J. Brickmann, and P. Läuger. 1981. Molecular dynamics study of ion transport in transmembrane protein channels. *Biophys. Chem.* 13:105–116.
7. Kappas, U., W. Fischer, E. E. Polymeropoulos, and J. Brickmann. 1985. Solvent effects in ionic transport through transmembrane protein channels. *J. Theor. Biol.* 112:459–464.
8. Aityan, S. K., and Y. A. Chizmadgev. 1984. A molecular dynamics study on water molecule movement in ionic channel. *Biol. Membr.* 1:901–912.
9. Mackay, D. H. J., P. H. Berens, K. R. Wilson, and A. T. Hagler. 1984. Structure and dynamics of ion transport through gramicidin A. *Biophys. J.* 46:229–248.
10. Kim, K. S., H. L. Nguyen, P. K. Swaminathan, and E. Clementi. 1985. Na^+ and K^+ ion transport through a solvated gramicidin A transmembrane channel: molecular dynamics studies using parallel processors. *J. Phys. Chem.* 89:2870–2876.
11. Rosenberg, P. A., and A. Finkelstein. 1978. Interaction of ions and water in gramicidin A channels. Streaming potentials across lipid bilayer membranes. *J. Gen. Physiol.* 72:327–340.
12. Levitt, D. G. 1983. Kinetics of movement in narrow channels. Ion channels: molecular and physiological aspects. *Curr. Top. Membr. Transp.* 19:244–280.
13. Rosenberg, P. A., and A. Finkelstein. 1978. Water permeability of gramicidin A-treated lipid bilayer membranes. *J. Gen. Physiol.* 72:341–350.
14. Schäfer, L., and A. Klemm. 1976. The pressure in molecular dynamics simulations of ionic liquids. *Z. Naturforsch.* A31:1068–1072.
15. Urry, D. W. 1972. A molecular theory of ion-conducting channels: a field-dependent transition between conducting and nonconducting conformations. *Proc. Natl. Acad. Sci. USA.* 69:1610–1614.
16. Wallace, B. A., W. R. Veatch, and E. R. Blout. 1982. The effects of lipid environment, ion-binding and chemical modifications on the structure of the gramicidin transmembrane channel. *Biophys. J.* 37:197–199.
17. Wallace, B. A. 1984. Ion-bound forms of the gramicidin A transmembrane channel. *Biophys. J.* 45:114–116.
18. Naik, V. M., and S. Krimm. 1984. Vibrational analysis of the structure of cristalline gramicidine A. *Biophys. J.* 45:109–112.
19. Henderson, D. 1974. Theory of simple mixtures. *Annu. Rev. Phys. Chem.* 25:461–483.
20. Jorgensen, W. L., J. Chandrasekhar, J. D. Madura, R. W. Impey, and M. L. Klein. 1983. Comparison of simple potential functions of simulating liquid water. *J. Chem. Phys.* 79:926–935.
21. Bounds, D. G., and P. J. Bounds. 1983. Potential surfaces derived from gradient calculations. New potentials for Li^+/H_2O, Na^+/H_2O, and K^+/H_2O. *Mol. Phys.* 50:25–32.
22. Bounds, D. G. 1985. A moelcular dynamics study of the structure of water around the ions Li^+, Na^+, K^+, Ca^{++}, Ni^{++} and Cl^-. *Mol. Phys.* 54:1335–1355.
23. Clementi, E., and H. Popkie. 1972. Study of the structure of molecular complexes. I. Energy surface of a water molecule in the field of a Lithium positive ion. *J. Chem. Phys.* 57:1077–1094.
24. Kistenmacher, H., H. Popkie, and E. Clementi. 1973. Study of the structure of molecular complexes. II. Energy surfaces for a water molecule in the field of a sodium or potassium cation. *J. Chem. Phys.* 58:1689–1699.
25. Dacre, P. D. 1984. The interaction of a water molecule with an ion at a distance. *J. Chem. Phys.* 80:5677–5683.
26. Dacre, P. D. 1984. SCF potential surfaces and derived models for Na^+ and Cl^- ions interacting with a water molecule. *Mol. Phys.* 51:633–659.
27. Vesely, F. 1978. Computerexperimente an Flüssigkeitsmodellen. Physik-Verlag, Weinheim. 160 pp.
28. Kushick, J., and B. J. Berne. 1977. Molecular dynamics method: continuous potentials. *In* Statistical Mechanics B. B. J. Berne, editor. Plenum Press, New York. 259 pp.
29. Streett, W. B., D. J. Tildesley, and G. Saville. 1978. Multiple time step methods and an improved potential function for molecular dynamics simulations of molecular liquids. *Am. Chem. Soc. Symp. Ser.* 86:144–158.
30. Szász, Gy. I., and K. Heinzinger. 1979. A molecular dynamics study of aqueous solutions. VIII. Improved simulation and structural properties of a NH_4Cl solution. *Z. Naturforsch.* 34*a*:840–849.
31. Gear, C. W. 1966. The numerical integration of ordinary differential equations of various orders. AEC Research and Development Report No. ANL-7126.
32. Evans, D. J. 1977. On the representation of orientation space. *Mol. Phys.* 34:317–325.
33. Evans, D. J., and S. Murad. 1977. Singularity free algorithm for molecular dynamics simulation of rigid polyatomics. *Mol. Phys.* 34:327–331.
34. Sonnenschein, R. 1985. An improved algorithm for molecular dynamics simulation of rigid molecules. *J. Comput. Phys.* 59:347–350.
35. Skerra, A., and J. Brickmann. 1987. Simulation of voltage driven hydrated cation transport through narrow transmembrane channels. In press.
36. Polymeropoulos, E. E., and J. Brickmann. 1985. Molecular dynamics of transport through transmembrane model channels. *Annu. Rev. Biophys. Biophys. Chem.* 14:315–330.
37. Dwivedi, A. M., and S. Krimm. 1984. *Biopolymers.* 23:923.
38. Fischer, W., and J. Brickmann. 1982. Lennard-Jones (12,6) parameters for the nonionic contributions to interionic pairpotentials of alkali cations and halide anions from crystal data. *Ber. Bunsen-Ges. Phys. Chem.* 86:650–656.